








Original Research

Ciprofol Regulates the Activity of Mitochondrial Respiratory Chain Complex I During Cerebral Ischemia-Reperfusion by Targeting Flavin Mononucleotide: A Metabolomic Study

Jixin Chen^{1,†}, Guoyou Chen^{2,†}, Yueheng Wu³, Shuai Liu¹, Yifan Ma⁴,
Maonan Liu¹, Wei Yu^{1,*}

¹Department of Anesthesiology, The Fourth Affiliated Hospital of Harbin Medical University, 150001 Harbin, Heilongjiang, China

²Daqing Campus College of Pharmacy, Harbin Medical University, 163319 Daqing, Heilongjiang, China

³Department of Anesthesiology, The First Affiliated Hospital of Baotou Medical College, Inner Mongolia University of Science and Technology, 014010 Baotou, Inner Mongolia, China

⁴Department of Anesthesiology, Tsinghua Chang Gung Hospital, 102200 Beijing, China

*Correspondence: [yuwei0123@163.com](mailto:yuweio123@163.com) (Wei Yu)

†These authors contributed equally.

Academic Editor: Hahn Young Kim

Submitted: 29 April 2025 Revised: 27 June 2025 Accepted: 4 July 2025 Published: 26 August 2025

Abstract

Background and Purpose: Ciprofol, a novel intravenous anesthetic, has been shown to exert protective effects against ischemic stroke, a leading cause of death and disability; however, its molecular mechanisms remain unclear. This study aimed to explore the molecular mechanisms underlying the neuroprotective effects of ciprofol using metabolomics. **Methods:** This study used a middle cerebral artery occlusion (MCAO) rat model to simulate cerebral ischemia-reperfusion injury (CIRI). The rats were divided into ciprofol, MCAO, and sham groups. Histological and neurobehavioral testing methods were used to investigate the therapeutic effects of ciprofol in rats. Ultra-high-performance liquid chromatography-quadrupole time-of-flight mass spectrometry was used to screen for differential metabolites and related metabolic pathways in the serum and brain of the three groups. Spectrophotometry was used to detect *in vitro* mitochondrial respiratory chain complex I (MRCC-I) activity. **Results:** Neurological behavioral scores and cerebral infarct volumes of rats in the ciprofol group were significantly lower than those of rats in the MCAO group. Metabolomic analysis revealed 19 differential metabolites in serum samples and 31 differential metabolites in brain samples, including flavin mononucleotide (FMN). These metabolites were mainly enriched in the tricarboxylic acid cycle, respiratory electron transport chain, and amino acid and lipid metabolism. *In vitro* experiments demonstrated that ciprofol promoted the activity of MRCC-I during CIRI by increasing FMN levels. **Conclusion:** The mechanisms of action of ciprofol during treatment of cerebral ischemia involve the tricarboxylic acid cycle, respiratory electron transport chain, and amino acid and lipid metabolism and may directly affect MRCC-I activity by regulating FMN.

Keywords: cerebral ischemia; mitochondrial complex I; flavin mononucleotide; metabolomics

1. Introduction

Stroke is one of the leading causes of death and permanent disability worldwide [1,2]. Ischemic strokes, which account for approximately 80% of all strokes, are characterized by a reduction in cerebral blood flow and ischemia, which can lead to severe and irreversible damage [3]. Although reperfusion therapy can prevent further ischemia [4], tissue damage can worsen during the ischemia-reperfusion process, ultimately leading to disability or death [5,6]. Ciprofol, a novel intravenous anesthetic derived from a structural modification of propofol, has a rapid onset, high potency, and good safety profile [7], reducing anesthesia-related cardiovascular depression [8]. A recent study has shown that ciprofol alleviates the iron cell apoptosis induced by cerebral ischemia-reperfusion injury (CIRI) by promoting the nuclear factor erythroid 2-related factor 2/cystine/glutamate antiporter/glutathione peroxidase 4 (Nrf2/XCT/Gpx4) signaling pathway, exerting a neuropro-

TECTIVE effect [9]. Although ciprofol has potential applications for the treatment of CIRI, its metabolic characteristics and molecular mechanisms remain unclear.

The impact of anesthetics on the body's metabolic spectrum is significant [10], and metabolic disturbances play a crucial role in CIRI [11,12]. In recent years, metabolomics has been used to investigate changes in the endogenous metabolites of complex biological systems and to identify potential biomarkers [13]. However, the relationship between the metabolic spectrum of the brain after CIRI, and to verify the its metabolites and signaling pathways, and the neuroprotective effects of ciprofol remain unclear. This study aimed to explore the influence of ciprofol on the metabolic spectrum of the brain following CIRI and to verify the possible mechanisms whereby it regulates its molecular target, flavin mononucleotide (FMN).



2. Experimental Methods and Materials

2.1 Reagents and Equipment

We used the following reagents during this study: ciprofol (Cat# H20200013, Liaoning Haisi Ke Pharmaceutical, Shenyang, Liaoning, China), 2,3,5-triphenyltetrazolium chloride (TTC) (Cat# T109275, Aladdin, Shanghai, China), pentobarbital sodium (Cat# BC076, Solarbio Science & Technology Company, Beijing, China), 4% paraformaldehyde fixative solution (Cat# P395744, Aladdin), formic acid (chromatography grade) (Cat# F433212, Aladdin), acetonitrile (chromatography grade) (Cat# A104440, Aladdin), glycerol (Cat# G116214, Aladdin), sucrose (Cat# S112226, Aladdin), HEPES-Tris (Cat# H109407, Aladdin), KCl (Cat# P122134, Aladdin), EGTA (Cat# E104434, Aladdin), NADH (Cat# N196977, Aladdin), BSA (Cat# D259432, Aladdin), protoporphyrin IX (Cat# F2420066, Aladdin), decylubiquinone (Cat# C463488, Aladdin), hexaammineruthenium(II) chloride (Cat# H282727, Aladdin), FMN (Cat# R106430, Aladdin), SF6847 (Cat# T129439, Aladdin), glutamic acid (Cat# G121400, Aladdin), succinic acid (Cat# S431423, Aladdin), trichloroacetic acid (Cat# T104257, Aladdin), mannitol (Cat# M108829, Aladdin), gentamicin (Cat# A132913, Aladdin) and potassium ferricyanide (Cat# P111567, Aladdin).

We used the following equipment and software during this study: analytical balance (No. ZCK201708115, Mettler-Toledo, Columbus, OH, USA), silicon rubber plug (No. 40-3756, Doccol, Sharon, MA, USA), micropipettes (QH05656, Thermo Fisher Scientific, Waltham, MA, USA), benchtop centrifuge (No. 10895, Sigma-Aldrich, St. Louis, MO, USA), high-speed refrigerated centrifuge (No. LC-2019-002, Sigma-Aldrich), ultra-pure water system (No. 201100078, Millipore, Billerica, MA, USA), 4 °C refrigerator, -20 °C freezer, -80 °C ultra-low temperature freezer (No. BH03G009400TXL8CDGCD, Haier, Qingdao, Shandong, China), disposable vacuum blood collection tube (No. WHB-30-1, Shanghai WoHong Biological Technology Co., LTD, Shanghai, China), ultra-high-performance liquid chromatography-quadrupole time-of-flight mass spectrometry (UPLC-Q/TOF-MS) (No. LC-MS110502, Waters, Milford, MA, USA), mass spectrometer TSQ8000 (No. LC-MS100702, Thermo Fisher Scientific), microinjection pump (No. 6132301008519, Shenzhen Maiketian Biomedical Technology Co., Ltd., Shenzhen, Guangdong, China), MassLynx software (version 4.1, Waters), Image-Pro Plus software (version 5.0, Media Cybernetics, Rockville, MD, USA), SPSS software (version 20.0, International Business Machines Corporation, Chicago, IL, USA), SIMCA-P software (version 11.5, Sartorius, Gottingen, Germany), vortex mixer (Serial No. 5426YN331111, Eppendorf, Hamburg, Germany), and scanner (Serial No. X6LW004066, Epson, Suwa, Japan).

2.2 Animal Preparation and Experimental Groups

Specific pathogen-free male Sprague–Dawley rats, weighing 210–230 g, were purchased from Changchun Yisi Experimental Animal Technology (Changchun, Jilin, China). The experimental animals were housed in the Central Laboratory of the Fourth Affiliated Hospital of Harbin Medical University throughout the experiment, with a temperature of 22 ± 2 °C, a relative humidity of $55\% \pm 5\%$, and a light-dark cycle of 12 h each day. All animals were fed standard food and allowed free access to water. The animals were acclimated to the rat facility for 7 days before the experiment. Adult male rats were randomly divided into a ciprofol group, a middle cerebral artery occlusion (MCAO) group, and a Sham group. During the experiment, all animals were provided with proper feeding and care according to relevant standards, and this experiment was approved by the Animal Ethics Committee. All experiments were conducted in accordance with relevant guidelines and regulations.

2.3 Establishment of a Rat MCAO and Reperfusion Model

A rat MCAO model was established with reference to the modified Zea Longa method to simulate CIRC [14]. Rats were anesthetized by intraperitoneal injection of 2% pentobarbital sodium (50 mg/kg) and fixed in the supine position. A silicon rubber plug was inserted from the proximal end of the external carotid artery (ECA) to occlude the origin of the middle cerebral artery (reperfusion was confirmed by laser Doppler). Ninety minutes later, the plug was gently removed, the ECA was completely ligated. The sham surgery group only underwent incision and suturing of the neck without any other procedures.

2.4 Drug Pump Infusion

After removing abdominal hair and disinfecting with iodine, the femoral vein was separated on one side of the rat, a puncture was made with a disposable intravenous puncture needle, and a catheter was placed and connected to an extension tube. Ciprofol was injected into the femoral vein using a microinjection pump at a rate of 9 mg/kg/h starting after successful placement of the catheter in the rat vein and lasting for 2 h until the time of removing the plug. Rats in other groups were infused with physiological saline at a rate of 9 mg/kg/h [15].

2.5 Neural Behavioral Testing

After 24 h, a neurobehavioral evaluation was performed. Using the modified Garcia test, the following six parameters were tested and recorded: reperfusion spontaneous activity, symmetry of limb movements, forelimb extension, climbing, body proprioception, and response to whisker touch. The neurobehavioral scores of each group of rats were recorded according to an 18-point neurological scoring criteria [16].

2.6 Measurement of the Cerebral Infarction Area

After 24 h of reperfusion, the rats were euthanized by decapitation after intraperitoneal injection of 2% pentobarbital sodium and whole brain tissues were removed. Brain tissues were frozen at -20°C for approximately 20 min. Then, the brain was sliced into six coronal sections on an ice block, with each slice being approximately 2-mm thick, and immersed in a 2% TTC solution at 37°C for 15 min. The volumes of the white areas of brain slices were calculated using Image-Pro Plus software, with the results representing the volume of cerebral infarction [17].

2.7 Metabolomic Analysis

2.7.1 Sample Preprocessing

The serum and ischemic brain hemispheres of rats in the Sham ($n=6$), MCAO ($n=6$), and ciprofol ($n=6$) groups were subjected to metabolomic analysis. First, 1050 μL of anhydrous methanol was used to extract 350 μL of samples, which were then vortexed for 1 min and centrifuged at 12,000 rpm for 12 min at 4°C in a high-speed, refrigerated centrifuge. The supernatant was then transferred to a new centrifuge tube using a micropipette and evaporated under a vacuum. The resulting samples were dissolved in a mixture of water and acetonitrile and were centrifuged again using the same method to obtain the final test samples [17].

2.7.2 Chromatographic Separation Conditions

This study used a UPLC system for chromatographic separation of samples. The mobile phase consisted of 0.1% formic acid (part A) and acetonitrile (part B) in water. For gradient elution, 100% part B was maintained for 2 min, then linearly changed to 80% part B within 10 min and maintained for 3 min, then linearly changed to 0% part B within 15 min and maintained for 5 min, finally linearly changed to 100% part B within 1 min and maintained for 4 min. The temperature of the automatic sampler was set at 4°C . The sample volume for each run was 5 μL . The eluate from the chromatographic column was directly analyzed using mass spectrometry [17].

2.7.3 Mass Spectrometry

A UPLC-Q/TOF-MS was used to detect metabolites eluted from the column. It was operated in electrospray ionization (ESI+) and negative ion (ESI-) modes, with a capillary voltage of 3.0 kV, an ion source temperature of 120°C , a desolvation temperature of 350°C , a sampling cone voltage of 30 V, nitrogen desolvation, and standard settings for positive and negative ion mode spray voltage fluctuations and collision energy. The survey was completed in 150 ms.

2.7.4 Data Processing and Statistical Analysis

MS data were imported into MassLynx software for further preprocessing, including peak detection and alignment. Each ion was identified by combining the retention time and m/z data. All data were normalized to the total

ion intensity of each chromatogram. Subsequently, the resulting data matrix was subjected to principal component analysis and multivariate partial least squares discriminant analysis (PLS-DA) using R (R Foundation, Vienna, Austria).

Before PLS-DA, all variables obtained from the UPLC-MS dataset were centered around the mean and scaled to Pareto variance. The results were subjected to 200 random permutations and response permutation testing (RPT) using SIMCA-P software to assess for the presence of overfitting in the unsupervised PLS-DA model and evaluate its overall robustness. Variable importance in projection (VIP) values were used to weight the sum of the PLS weights, reflecting the relative contribution of each variable to the model. The criteria for selecting differentially expressed metabolites in this study were a VIP value in the top 50 and a p -value of <0.05 [17].

2.7.5 Key Metabolites and Metabolic Pathways

The metabolites were detected using UPLC-Q/TOF-MS, with the identification method determining the elemental composition of the corresponding compounds within the error range. The HMDB and Reactome databases were used to identify differential metabolites and metabolic pathways [17].

Metabolites that have a significant impact on metabolic pathways and can cause significant changes in the plasma or brain tissues of MCAO rats were identified as potential biomarkers. Metabolic pathway enrichment results were obtained using Reactome for further analysis. The number of Reactome pathways enriched with significantly differentially expressed metabolites was determined using hypergeometric testing.

2.8 Preparation of Extracellular Mitochondrial Membrane

Differential centrifugation was used to separate mitochondrial membranes from frozen brain hemispheres. After a frozen intact brain was divided into two hemispheres along the sagittal plane, the brain cortex with the most damage was separated from the posterior to the anterior, including the cortical and striatal areas. The brain tissue was then stored in a -80°C freezer. Frozen brain tissue was added to a homogenizer containing 10 mL of isolation buffer mannitol/sucrose/ethyleneglycol-bis (b-aminoethyl ether)-N,N,N,N'-tetraacetic acid (EGTA) medium (MSE) (225 mmol/L mannitol, 75 mmol/L sucrose, 20 mmol/L 4-(2-Hydroxyethyl)-1-piperazineethanesulfonic acid-Tris (HEPES-Tris), 1 mmol/L Ethylene glycol-bis(2-aminoethylether)-N,N,N,N'-tetraacetic acid (EGTA), 1 mg/mL Bovine Serum Albumin (BSA), pH 7.4) with 80 $\mu\text{g/mL}$ of penicillin and homogenized 60 times to release low molecular weight metabolites. After centrifugation at 1500 g for 5 min at 4°C to remove tissue fragments, the supernatant was centrifuged at 20,000 g for 15 min at 4°C and washed twice with MSE buffer without BSA. The

final pellets are suspended in 60 μ L of the same buffer and stored at -80°C until use [18].

2.9 Measurement of Mitochondrial Membrane MRCC-I Activity

Mitochondrial respiratory chain complex I (MRCC-I) activity was determined by spectrophotometry at 25°C using a microplate reader in 0.2 mL of buffer (125 mmol/L KCl, 20 mmol/L HEPES-Tris, 0.02 mmol/L EGTA, pH 7.6) [19]. The activity of MRCC-I at 0.15 mM of NADH was measured at 340 nm in a buffer containing 40 $\mu\text{g/mL}$ of gentamicin and 1 mM of potassium ferricyanide (NADH culture medium). NADH: Q reductase was measured in a NADH culture medium containing 2 mg/mL BSA, 60 $\mu\text{mmol/L}$ decylubiquinone, and mitochondrial protein. NADH: HAR reductase was detected in the NADH culture medium containing 1 mM HAR and mitochondrial proteins.

2.10 Data Analysis

All data were analyzed using SPSS software. The Shapiro-Wilk test was used to check whether the data were normally distributed. Neurobehavioral test scores were compared using the Wilcoxon matched pair signed rank test. In addition, one-way analysis of variance was performed for comparisons of more than two groups, followed by Tukey's test. For the comparison of mitochondrial complex I enzyme activity between different groups, multiple *t*-tests with false discovery rate (FDR) correction for multiple comparisons were used. The normally distributed data are presented as the mean \pm standard error of the mean, and neurobehavioral scores are shown as the median, 25th percentile, 75th percentile, and minimum and maximum values in the box plot. Statistical significance was set at $p < 0.05$, with one, two, and three asterisks representing significance levels below 0.05, 0.01, and 0.001, respectively.

3. Results

3.1 The Protective Effect of Ciprofol on CIRI in Rats

The experimental schedule is shown in Fig. 1A. Thirty minutes before blocking the MCA, ciprofol administration was commenced at a rate of 9 mg/kg/h through a pump for a total duration of 2 h. Various indicators were tested after 24 h of cerebral reperfusion. The results showed that the ischemic stroke volume percentage of the MCAO group was $28.6 \pm 4.1\%$, whereas it was $20.3 \pm 3.0\%$ in the ciprofol group (Fig. 1B,C), with a significant difference between the two groups ($p < 0.01$). Compared to the Sham group, the neurological behavioral scores of rats in the MCAO group were significantly lower ($p < 0.001$), whereas the neurological behavioral scores of rats in the ciprofol group were significantly higher than those in the MCAO group (Fig. 1D) ($p < 0.001$). These results indicate that ciprofol treatment significantly alleviated the neurofunctional damage induced by cerebral ischemia-reperfusion.

3.2 Multivariate Statistical Analysis of Metabolites

This study used UPLC-Q/TOF-MS for metabolomic analyses of serum and brain tissue samples. To further investigate the similarities and differences between the Sham, MCAO, and ciprofol groups, we constructed a PLS-DA model that is widely used in metabolomics research. Based on the PLS-DA plots, we found clear separation trends in the serum (Fig. 2A) and brain (Fig. 2B) tissues of the three groups of rats, indicating good precision and reproducibility of the metabolomic data. The plots clearly show two main components of serum, PC1 (30.1%) and PC2 (25.1%), and two independent components of the brain, PC1 (37.7%) and PC2 (11.9%), suggesting a significant effect of ciprofol treatment. The serum samples achieved $R^2 Y$ and Q^2 values of 0.492 and -0.984 , respectively, in the PLS-DA score plots, whereas the brain samples had $R^2 Y$ and Q^2 values of 0.331 and -1.014 , indicating the good fit and reliability of the model. Additionally, this study used RPT to assess the model quality, with the green regression line of Q^2 points intersecting below zero on the left side of the vertical axis, further validating the effectiveness of the model (Fig. 2C,D).

3.3 Differential Expression of Substance Identification

Research findings have shown that ciprofol causes significant changes in a variety of metabolites during the treatment of MCAO rats. To explore the biological significance of these metabolites in ciprofol-treated MCAO rats, we identified three groups of metabolites with significant differences. Previous studies have indicated that variables with VIP values of >1 have a significant impact on the separation of samples in PLS-DA and can be used as criteria for screening for differential metabolites [17,20]. However, no study has confirmed a causal relationship between these screened differential metabolites and cerebral ischemia injury. For example: erucamide, lathosterol, and threonate, among others. Therefore, the selection criteria used in this study were a top-50 VIP value and $p < 0.05$.

Based on these screening criteria, we identified 19 differential metabolites in the serum of the Sham, MCAO, and ciprofol groups (Table 1). To comprehensively demonstrate the relationships between these three groups of samples and the differences in the expression patterns of these metabolites, we used a hierarchical clustering analysis to determine the quality and intensity of these differential compounds. The cluster heatmap showed variations in FMN metabolites between the serum sample groups, with color changes reflecting the overall changes in metabolites (Fig. 3A). Compared to those in the Sham group, the levels of lysophosphatidylethanolamine (LPE), 1-O-hexadecyl-SN-glycero-3-phosphocholine (lyso-PAF C-16), phosphatidylethanolamine (PE), sphinganine, and L-carnitine were significantly increased in the MCAO group. In contrast, the levels of these metabolites were lower in the ciprofol group than in the MCAO group. Additionally, cit-

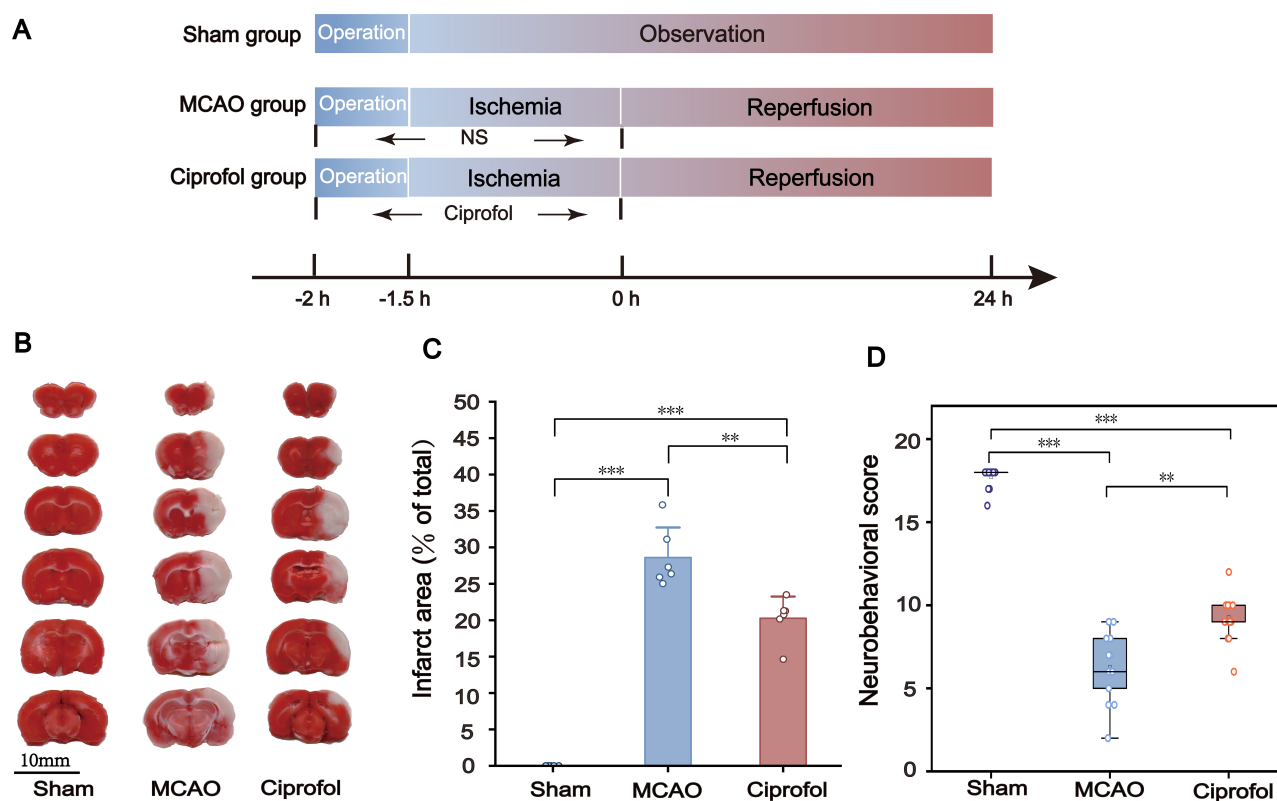


Fig. 1. Neuroprotective effects of ciprofol on cerebral ischemia-reperfusion. (A) Schematic diagram of the experimental timeline. (B) Representative TTC-stained images of the brain at 24 h after middle cerebral artery occlusion and reperfusion. The scale bar = 10 mm. (C) Quantitative analysis of infarct volume (n = 6, F (2,15) = 150.170, $p = 0.0000000001$). (D) Comparison of neurological behavioral scores at 24 h after reperfusion. Values are presented as the mean \pm standard deviation (n = 12) (** $p < 0.01$, *** $p < 0.001$). MCAO, middle cerebral artery occlusion; TTC, 2,3,5-triphenyltetrazolium chloride; NS, normal saline.

rate, succinate, lysophosphatidylcholine (LPC), and deoxycholic acid levels showed a downward trend in the MCAO group, whereas the levels of these metabolites were further decreased in the ciprofol group.

The analysis of brain tissue sampled from the three groups of rats revealed differences in the presence of 31 metabolites (Table 2). The clustered heat map (Fig. 3B) illustrates the changes in metabolites in the brain tissue samples. Compared to the Sham group, the levels of aspartate, N-acetylaspargate (NAA), N-acetylaspargylglutamate (NAAG), 4-hydroxyisoleucine, FMN, and pyruvate were lower in the brain tissues of rats in the MCAO group, whereas ciprofol reversed the decreases in these metabolites in the brain tissues of rats in the MCAO group.

We then analyzed linear correlations between different metabolites in the serum and brain samples by calculating Pearson correlation coefficients and conducting statistical tests for p -values. The correlation analysis results for serum metabolites (Fig. 4A) showed that citric acid, pyruvate, and lipids were highly positively correlated with lipid substances. Correlation analysis results for different brain metabolites (Fig. 4B) indicated that pyruvate and FMN had high positive correlations with lipid and amino acid metabo-

lites. However, the correlation between succinic acid and the other metabolites was weaker. This finding suggests that citric acid, pyruvate, FMN, lipid substances, and amino acid metabolites play important roles in the neuroprotective effects of ciprofol in MCAO rats.

3.4 Metabolic Pathway Analysis

To explore the potential protective mechanisms of ciprofol against CIRI, differential metabolites were used to construct metabolic pathways. According to the Reactome enrichment analysis, of the 20 pathways with the smallest p -values in the three groups of rat serum samples, the key metabolic pathways for neuroprotection by ciprofol (Fig. 5A) were the tricarboxylic acid cycle, pyruvate metabolism, and mitochondrial respiratory chain. Pathways in brain tissue samples (Fig. 5B) also included steroid metabolism, as well as pathways for aspartate and glutamate metabolism. There was a clear correspondence between the enriched differential metabolites and metabolic pathways in the three groups of rats, with citric acid being involved in the tricarboxylic acid cycle, pyruvate metabolism, and mitochondrial respiratory chain; pyruvate being involved in pyruvate metabolism and tricar-

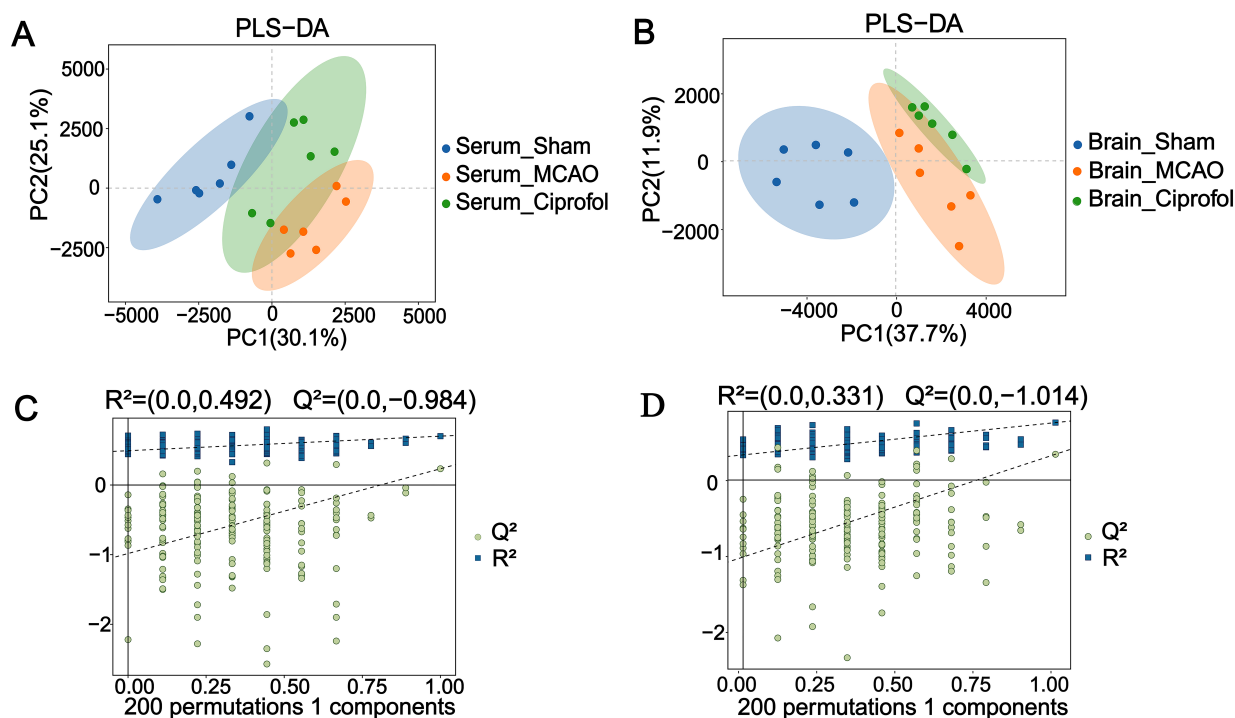


Fig. 2. Multivariate statistical analyses of serum and brain tissue metabolomic data. (A) PLS-DA of serum samples. (B) PLS-DA of brain tissue samples. (C) RPT plot of the PLS-DA model for serum samples. (D) RPT plot of the PLS-DA model for brain tissue samples. PLS-DA, partial least squares discriminant analysis; RPT, response permutation testing.

boxylic acid cycle processes; and FMN being associated with the tricarboxylic acid cycle and mitochondrial respiratory chain.

To clarify the potential mechanisms, we correlated important metabolic pathways with differential metabolites, presenting a comprehensive analysis of the effects of ciprofol on metabolic processes in MCAO rats (Fig. 6). The citric acid cycle links pyruvate metabolism and mitochondrial respiratory chain pathways. Compared with the Sham group, the FMN content of the brain tissue samples of the ciprofol group were significantly downregulated, and the MCAO group showed a further significant downregulation of FMN content, indicating that ciprofol regulates FMN content in the brains of MCAO rats.

3.5 Mitochondrial Membrane MRCC-I Activity

MRCC-I activity in rats with cerebral ischemia-reperfusion is closely related to CIRI. To detect MRCC-I activity in the mitochondrial membrane, we examined the effects of different concentrations of ciprofol. The results showed that, after treatment with ciprofol at concentrations of 25, 50, and 100 $\mu\text{mol/L}$ [21], the activities of the Q enzyme and hexaammineruthenium (HAR) reductase of MRCC-I were significantly increased (Fig. 7A,B). Within 4 h, the Q-reductase activity showed a concentration-dependent increase with increasing concentrations of ciprofol. Within 1 h, the activity of HAR reductase increased with the concentration of ciprofol; however, after 1h, cipro-

fol at 25- $\mu\text{mol/L}$ demonstrated higher activity compared to the 50- $\mu\text{mol/L}$ concentration. These findings indicate that ciprofol enhances the activity of MRCC-I after cerebral ischemia; however, the concentration dependence of HAR reductase changes after 1 h.

3.6 Ciprofol Inhibits the Activity of Reductase HAR by Regulating the Amount of FMN Bound to the Membrane, Suppressing Reverse Electron Transfer (RET)

Within a 15-min time period after pretreatment with 100 $\mu\text{mol/L}$ of ciprofol and without any other treatments, FMN was added, trichloroacetic acid was used as an FMN-dissociating agent, the Epidermal Growth Factor Receptor (EGFR) inhibitor, SF6847, was applied, and the activities of mitochondrial membrane Q and HAR reductase were determined (Fig. 8A,B). The results showed that, after treatment with 10 $\mu\text{mol/L}$ of FMN, the activities of both enzymes were upregulated. After removal of FMN from the mitochondrial membrane with trichloroacetic acid, the activities of both enzymes were significantly decreased in the FMN inhibitor group, which indicates that ciprofol modulates the amount of membrane-bound FMN. Under RET conditions, the activities of both enzymes were inhibited. In order to inhibit the RET state, the activity of Q reductase was higher than in the RET group, but lower than in the Control group after using the EGFR inhibitor, whereas the activity of HAR reductase was higher than in the Control group. This result indicates that inhibition of RET by ciprofol mainly affects the activity of HAR reductase.

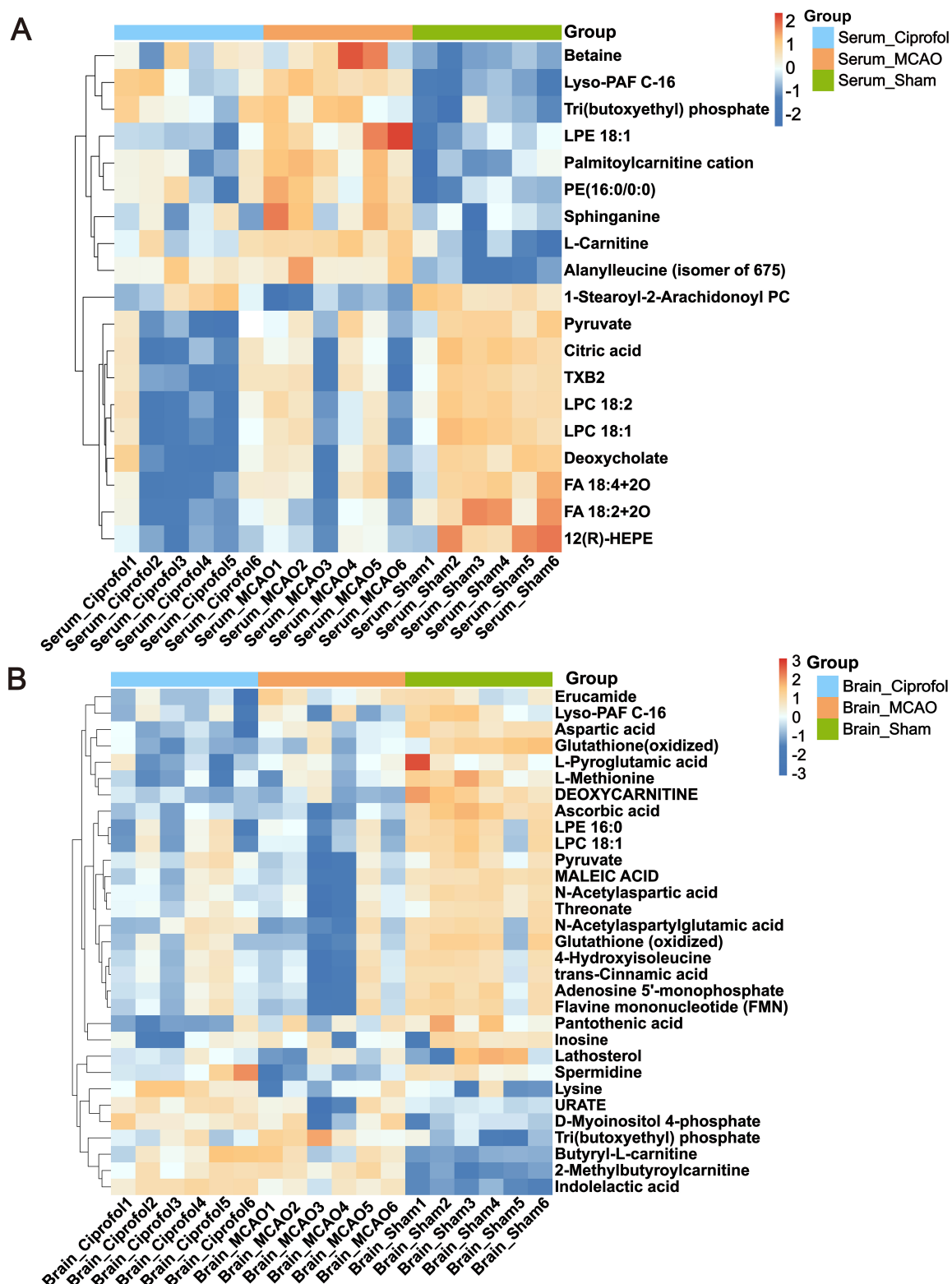


Fig. 3. Three sets of rat serum and brain tissue complex I sub-base FMN and differential metabolite clustering analyses. (A) Heat map of significantly expressed metabolites clustered in serum samples. **(B)** Heat map of FMN and other significantly expressed metabolites clustered in brain tissue samples. (Data standardized between -3 and 3 ; colors from blue to red indicate metabolite expression levels from low to high). FMN, flavin mononucleotide; lyso-PAF, lysophosphatidyl platelet-activating factor; LPE, lysophosphatidylethanolamine; PE, phosphatidylethanolamine; TXB2, thromboxane B₂; LPC, lysophosphatidylcholine; FA, fatty acid; 12(R)-HEPE, 12(R)-hydroxyeicosapentaenoic acid.

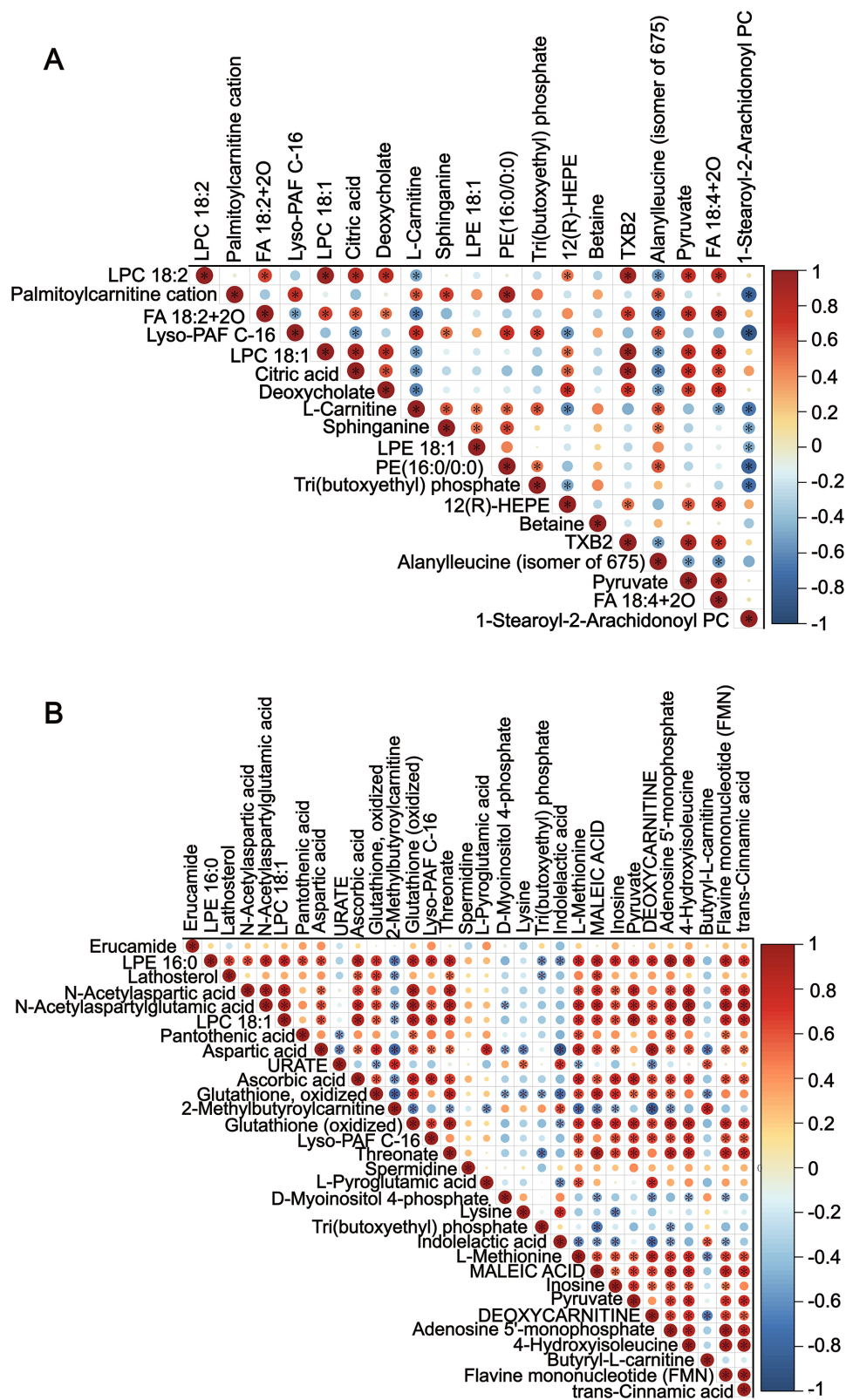


Fig. 4. Correlations between complex I cofactor FMN in the serum and brain tissue samples obtained from three groups of rats with differential metabolites. (A) Correlation map of significantly expressed metabolites in serum samples. (B) Correlation map of FMN and other significantly expressed metabolites in brain tissue samples. (The highest correlation coefficient is 1 (red), indicating complete positive correlation, while the lowest correlation coefficient is -1 (blue), indicating complete negative correlation. The blank part in the figure represents $p > 0.05$ from the correlation statistical test, while the colored part represents $p < 0.05$).

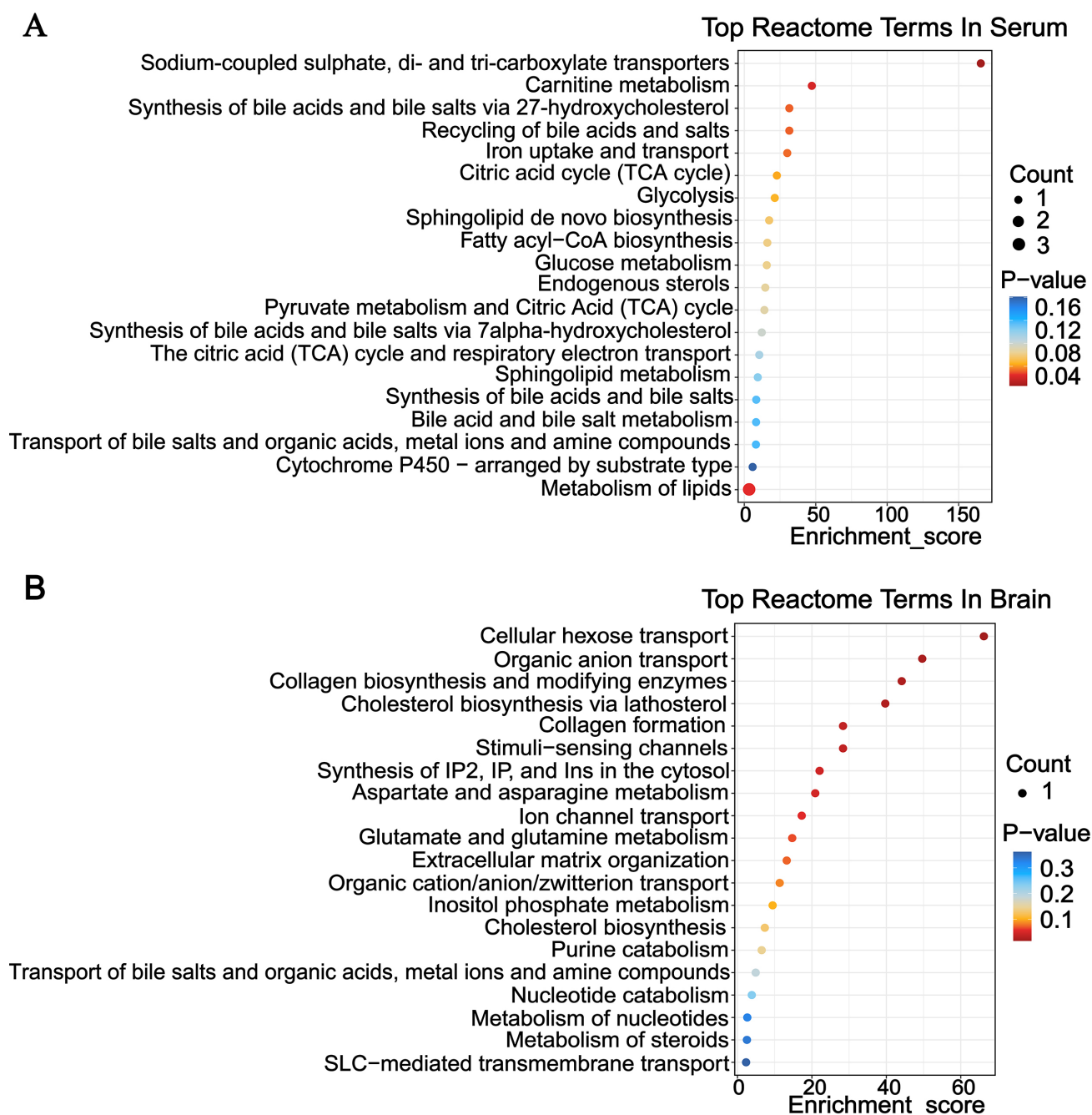


Fig. 5. Enrichment analysis of rat serum and brain tissue samples obtained from the three groups, including the tricarboxylic acid cycle, mitochondrial respiratory chain, and other top 20 pathways. (A) Bubble plot of Reactome pathways in serum samples. (B) Bubble plot of Reactome pathways in brain tissue samples. Pathways with larger bubbles contain more different metabolites; the color of the bubbles changes from blue to red, with smaller enrichment p -values indicating greater significance. IP, inositol 1,4,5-trisphosphate; SLC, solute carrier.

4. Discussion

Ciprolol is a novel intravenous anesthetic with unique physical and chemical properties conferred by its cyclic structure, which involves the addition of a cyclopropyl group to the side chain of the 2,6-di-substituted phenol of propofol [22]. A previous study has shown that ciprolol may exert neuroprotective effects by modulating the antiox-

idant stress responses of neurons during cerebral ischemia-reperfusion [9]. However, the effects of ciprolol on cerebral metabolic pathways during ischemia-reperfusion remain unclear. Thus, this study provides new insights into the mechanisms underlying brain protection by ciprolol through metabolomics and the molecular target, FMN. Our results demonstrated that ciprolol affects the phospholipid

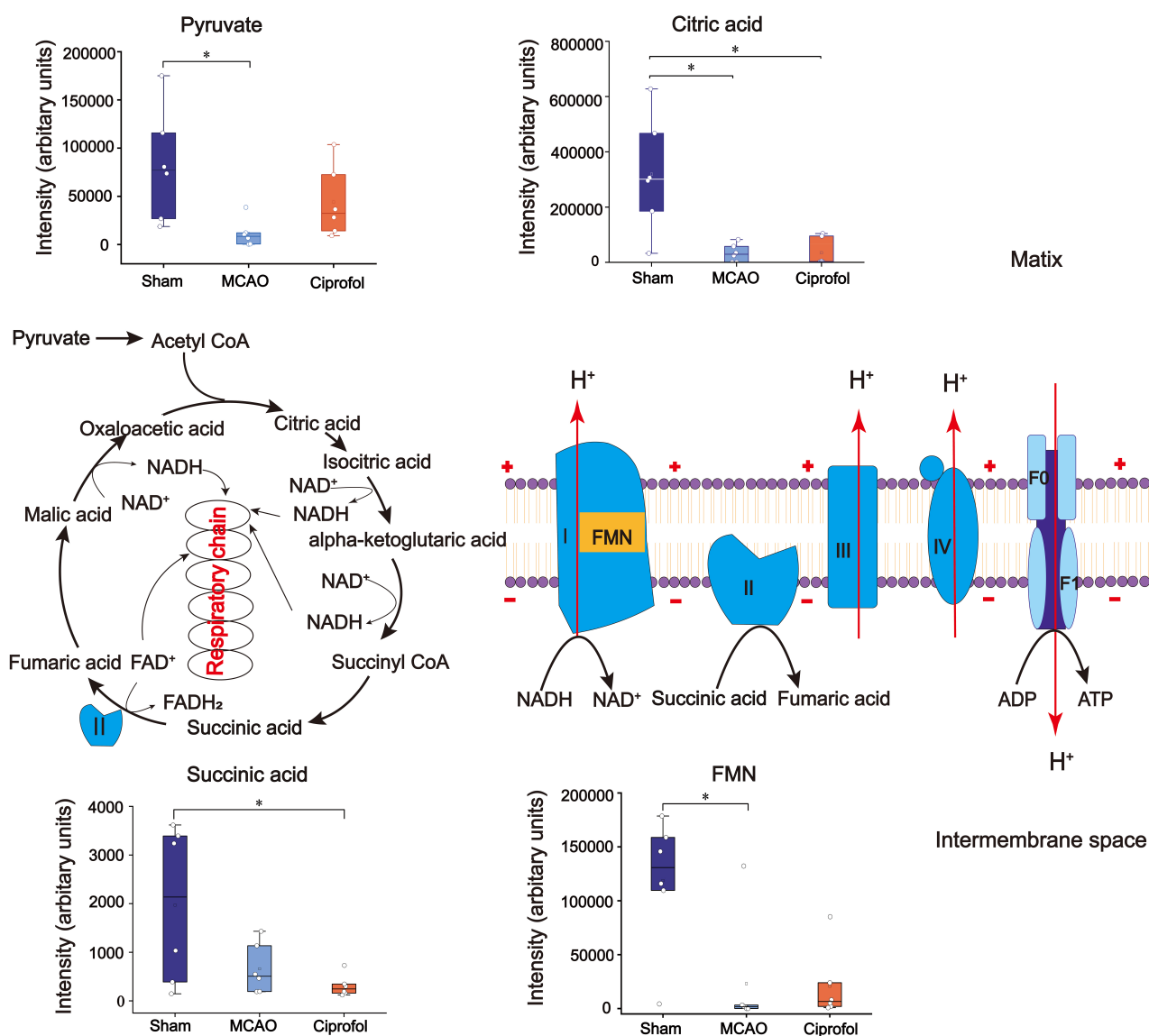


Fig. 6. Analysis of differential metabolites in the tricarboxylic acid cycle and mitochondrial respiratory chain pathway in the three groups of rats. Results of the Kruskal–Wallis test showing significant differences in succinic acid ($H(2) = 4.393, p = 0.0112$), citric acid ($H(2) = 8.433, p = 0.0148$), and pyruvate ($H(2) = 8.047, p = 0.0179$). Results of the Bonferroni correction showing significant differences in succinic acid (adjusted $p = 0.1317$, MCAO group vs. ciprofol group), citric acid (adjusted $p = 0.0128$, Sham group vs. MCAO group) and pyruvate (adjusted $p = 0.0148$, Sham group vs. MCAO group) (* $p < 0.05$).

metabolism pathway, tricarboxylic acid cycle, respiratory electron transport chain, and amino acid metabolism pathway in brains damaged by ischemia-reperfusion, potentially regulating the activity of MRCC-I after cerebral ischemia by modulating FMN, thereby exerting neuroprotective effects.

Ischemic brain injury can lead to metabolic pathway disorders, which, in turn, impair neurological function [23]. Our results showed that compared with the control group, the MCAO group had a significant increase in cerebral infarction volume and significant decrease in neurobehavioral scores. Amino acid metabolism, glycerol phospholipid metabolism, tricarboxylic acid cycle, mitochondrial oxida-

tion respiratory chain, and other pathways and metabolites in the MCAO group were significantly changed. This is consistent with the results of previous studies [24,25]. Changes in metabolic profiles may play an important role in the etiology and therapeutic targeting of various diseases. Studies have shown that potential therapeutic sites in the metabolic pathways of rat brains after cerebral ischemia-reperfusion include steroid metabolism, glycerophospholipid metabolism, alanine metabolism, aspartate and glutamate metabolism, the tricarboxylic acid cycle, and the respiratory electron transport chain [26–31].

Our study has found that enrichment values of the tricarboxylic acid cycle and mitochondrial oxidative respira-

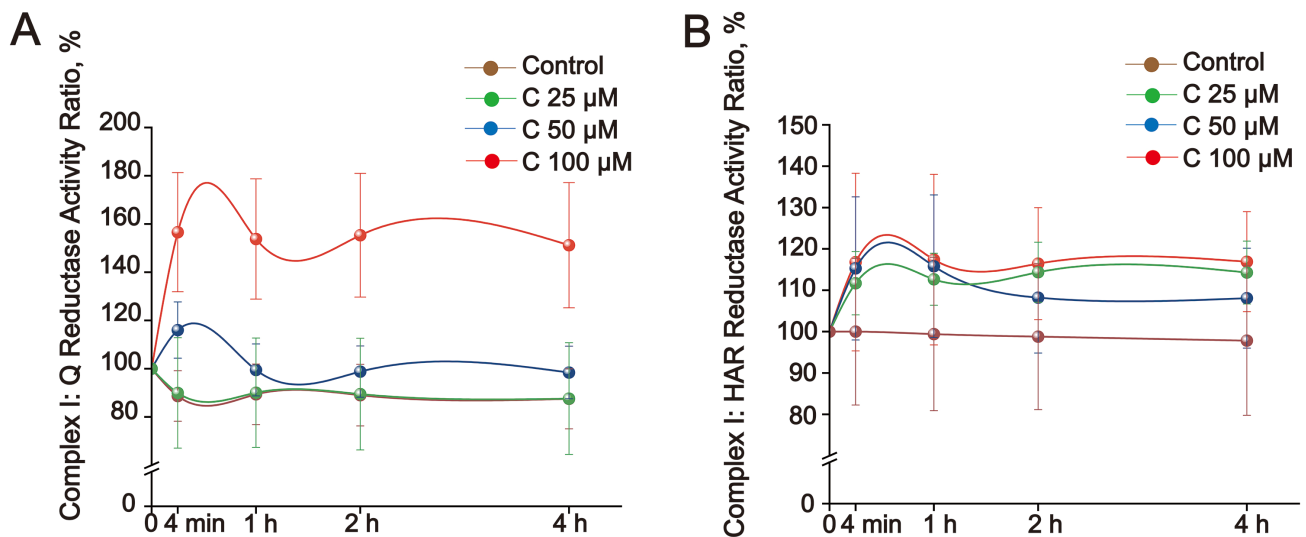


Fig. 7. The effect of ciprofol on the activity of MRCC-I after cerebral ischemia-reperfusion. (A) Q reductase activity ratio. (B) HAR reductase activity ratio. C 25 μ M, C 50 μ M, C 100 μ M represents 25, 50, and 100 μ mol/L ciprofol. HAR, hexaammineruthenium.

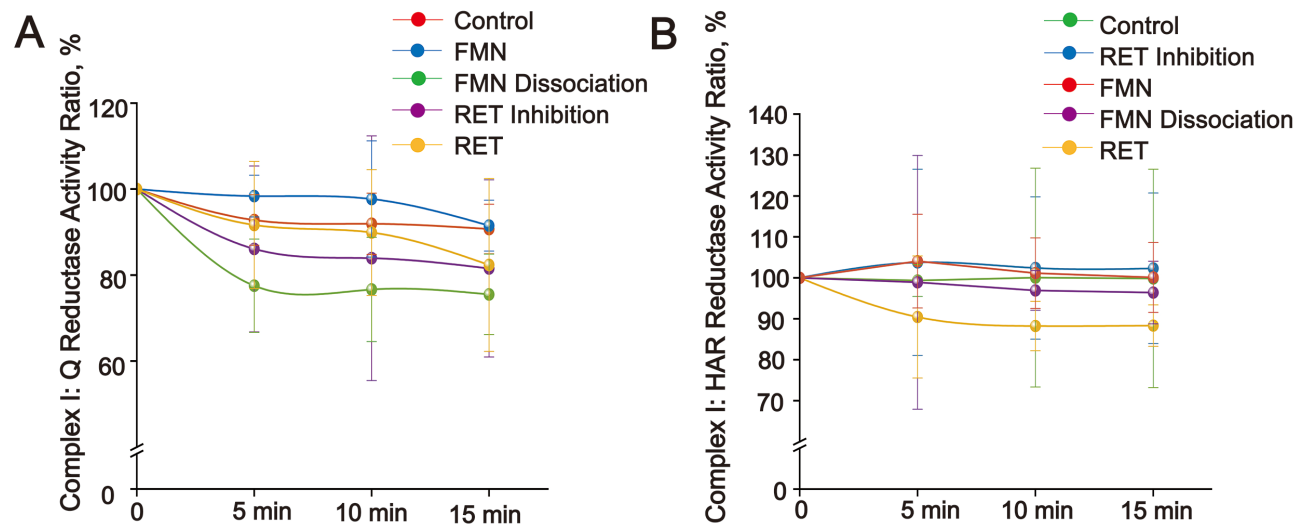


Fig. 8. Activities of MRCC-I under four conditions: RET, RET inhibition, FMN supplementation, and FMN dissociation. (A) Q reductase activity ratio. (B) HAR reductase activity ratio. FMN: 10 μ mol/L/FMN, FMN dissociation: 10% trichloroacetic acid. RET: 5 mmol/L succinic acid and 1 mmol glutamic acid. RET inhibition: 50 nmol/L SF6847. RET, reverse electron transfer.

tory chain were higher after a ciprofol intervention. One of the key mechanisms underlying CIRI is a disruption of energy metabolism [29]. The tricarboxylic acid cycle and mitochondrial respiratory chain are the main pathways for obtaining energy [32,33]. Dysfunction of these pathways during CIRI may lead to energy production disorders, resulting in brain tissue damage. Our results show that ciprofol can upregulate the content of FMN and downregulate the succinic acid content in these two pathways. A study has shown that ischemic brain injury leads to succinic acid accumulation in brain tissue, and, in the initial minutes of reperfusion, succinate dehydrogenase rapidly oxidizes these accumulated succinic acids to drive the production of superoxide in the mitochondria [34]. Therefore, reducing

ischemic succinate accumulation may alleviate CIRI in the brain. After 24 h of reperfusion, succinic acid metabolism may be normalized and the succinic acid level returned to baseline value due to the gradual recovery of Succinate dehydrogenase (SDH activity) [35]. The results of this study showed that after 24 h of reperfusion, there was no difference in succinic acid level in the MCAO group compared with that in the Sham group. This finding is consistent with that of previous studies. However, the VIP values of succinic acid in serum samples were low, indicating its limited importance. In contrast, FMN is a distinctly different metabolite. Non-valent binding of FMN to mitochondrial complex I may have a protective effect on ischemia-reperfusion brain. FMN deficiency complex I does not per-

Table 1. Differential metabolic substances in the brain between three groups.

Metabolite	VIP value	<i>p</i> -value
Erucamide	5.0291357	0.0497359
N-Acetylaspartic acid	4.8755229	0.0000344
Lathosterol	4.4977343	0.0337705
LPE 16:0	2.9807346	0.0049651
N-Acetylaspartylglutamic acid	2.7292153	0.0027227
LPC 18:1	2.3136287	0.0060075
Pantothenic acid	2.0607321	0.0143361
Aspartic acid	2.0025866	0.0000090
URATE	1.9211953	0.0211415
Ascorbic acid	1.8800543	0.0135255
Glutathione, oxidized	1.6330243	0.0001156
2-Methylbutyrylcarnitine	1.5984963	0.0026922
Glutathione (oxidized)	1.5712596	0.0008850
Lyso-PAF C-16	1.3892906	0.0355122
Threonate	1.3584918	0.0016951
Spermidine	1.3354016	0.0334715
L-Pyroglutamic acid	1.3103007	0.0465312
D-Myoinositol 4-phosphate	1.2319886	0.0356007
Lysine	1.1793463	0.0165820
Tri(butoxyethyl) phosphate	1.1726142	0.0045967
Indolelactic acid	1.0751668	0.0000130
L-Methionine	1.0576214	0.0009989
MALEIC ACID	1.0349934	0.0005902
Inosine	0.9474527	0.0380657
Pyruvate	0.9126423	0.0292241
DEOXYCARNITINE	0.8609674	0.0380656
Adenosine 5'-monophosphate	0.8217201	0.0016711
4-Hydroxyisoleucine	0.7987548	0.0032812
Butyryl-L-carnitine	0.7970167	0.0338654
Flavine mononucleotide (FMN)	0.7953430	0.0062147
trans-Cinnamic acid	0.7675618	0.0254009

Note: Differential metabolite VIP and *p* values among three groups of rat brain tissue samples. VIP, variable importance in projection.

form physiological NADH oxidation and does not promote energy production [36]. Upon reperfusion, the dissociated FMN can be rapidly re-oxidized by oxygen, producing an equimolar amount of hydrogen peroxide in the matrix and significantly leading to I/R-induced oxidative stress and tissue damage [19]. This leads us to speculate that it may be an important target for ciprofloxacin to alleviate CIRI [37,38].

Riboflavin is a biological precursor of FMN and flavin adenine dinucleotide (FAD), which play crucial roles in normal development, growth, reproduction, lactation, and overall health [39]. The human body cannot synthesize riboflavin on its own; instead, it must be obtained through dietary intake. After absorption in the intestine, riboflavin is transported to various tissues and cells via the riboflavin transporter (RFVT)/SLC52A), and its synthesis is regulated by riboflavin kinase and FAD synthetase [40]. FMN exists

Table 2. Differential metabolic substances in the serum between three groups.

Metabolite	VIP value	<i>p</i> -value
1-Stearoyl-2-Arachidonoyl PC	5.383391607	0.001416961
LPC 18:2	3.797437784	0.003617146
Palmitoylcarnitine cation	3.486276568	0.000458000
FA 18:2+2O	2.751816182	0.004745506
Lyso-PAF C-16	2.643654672	0.000231106
LPC 18:1	2.409469758	0.001830447
Citric acid	2.363239461	0.001501018
Deoxycholate	1.757289487	0.038394668
L-Carnitine	1.723285476	0.000162688
Sphinganine	1.368068147	0.008981335
LPE 18:1	1.337447676	0.028772132
PE(16:0/0:0)	1.295700045	0.002692241
Tri(butoxyethyl) phosphate	1.173439887	0.018705785
12(R)-HEPE	1.124474759	0.021640872
Betaine	1.071909219	0.049841179
TXB2	0.894726424	0.007038942
Alanylleucine (isomer of 675)	0.735835699	0.000620190
Pyruvate	0.731008846	0.023099686
FA 18:4+2O	0.711020642	0.011873160

Note: Differential metabolite VIP and *p* values among three groups of rat serum tissue samples.

in the mitochondria in free and membrane-bound forms and is essential for ATP and NADH generation [41]. ATP and NADH regulate mitochondrial function and alleviate neuronal cell death [42,43]. Therefore, FMN plays a crucial role in protecting the brain during ischemia-reperfusion. Rats treated with riboflavin exhibit a reduction in MRCC-I activity during brain ischemia/reperfusion, thereby decreasing the incidence of CIRI [18]. A study has suggested that, during brain ischemia-reperfusion, succinate-supported reverse electron flow leads to a dissociation of FMN from MRCC-I, resulting in decreased activity, which is considered a new mechanism of CIRI [44]. Our results show that ciprofol inhibits RET by regulating the amount of membrane-bound FMN, thereby enhancing HAR reductase activity. Additionally, riboflavin is associated with a protection of cognitive function, possibly due to its anti-inflammatory and antioxidant properties [45].

MRCC-I is a membrane-bound protein that contains noncovalently bound FMN and eight iron-sulfur proteins [46]. During cerebral ischemia-reperfusion, the amount of FMN bound to the mitochondrial membrane decreases, leading to decreases in MRCC-I activity [38]. Therefore, MRCC-I activity during cerebral ischemia-reperfusion is worthy of attention. Following ischemia-reperfusion, the activity of MRCC-I in the mitochondrial oxidative respiratory chain was most sensitive to its influence, whereas MRCC II-IV values were almost fully recovered at 1–6 h after reperfusion [47]. Reduced MRCC-I activity impairs electron chain transfer, disrupts energy balance, and affects

ATP synthesis, thereby affecting mitochondrial biogenesis and energy metabolism, which are closely related to the neuroprotective mechanism of cerebral ischemia [48]. Our study shows that ciprofol promotes MRCC-I activity after cerebral ischemia, with changes in the concentration dependency of HAR reductase occurring after 1 h. In addition, on the inner mitochondrial membrane, the electron transport chain generates a proton gradient through mitochondrial respiratory chain complexes to drive ATP synthesis [49].

5. Conclusions

Ciprofol affects phospholipid metabolism, the tricarboxylic acid cycle, the mitochondrial oxidative respiratory chain pathway, and amino acid metabolic pathways in the brains of rats with CIRI. Our study further verifies that ciprofol targets MRCC-I activity by regulating membrane-bound FMN content, which may be its specific molecular mechanism for brain protection.

Abbreviations

CIRI, cerebral ischemia-reperfusion injury; ECA, external carotid artery; FAD, flavin adenine dinucleotide; FMN, flavin mononucleotide; lyso-PAF C-16, 1-O-hexadecyl-SN-glycero-3-phosphocholine; LPC, lysophosphatidylcholine; LPE, lysophosphatidylethanolamine; MCAO, middle cerebral artery occlusion; MRCC, mitochondrial respiratory chain complex; MS, mass spectrometry; NAA, N-acetylaspartate; NAAG, N-acetylaspartylglutamate; PE, phosphatidylethanolamine; PLS-DA, partial least squares discriminant analysis; RET, reverse electron transfer; RPT, response permutation testing; SD, Sprague–Dawley; SPF, specific pathogen-free; UPLC-Q/TOF-MS, ultra-high-performance liquid chromatography-quadrupole time-of-flight ultra-high-performance liquid chromatography; VIP, variable importance in projection.

Availability of Data and Materials

The datasets used and analyzed during the current study are available from the corresponding author on reasonable request.

Author Contributions

WY—conception and design of the study; JXC, GYC and YFM—experimental implementation and data collection; WY, JXC, GYC, YHW, YFM, SL and MNL—analysis and interpretation of the data; JXC, YHW and GYC—manuscript drafting. All authors contributed to editorial changes in the manuscript. All authors read and approved the final manuscript. All authors have participated sufficiently in the work and agreed to be accountable for all aspects of the work.

Ethics Approval and Consent to Participate

The animal experimental protocol strictly follows the National Institutes of Health Animal Guidelines and has been approved by the Animal Ethics Committee of Harbin Medical University Fourth Hospital. The core standard followed in this study is the 3R principle (substitution, reduction, optimization), ARRIVE 2.0 guidelines, and the specific operation complies with the AAALAC (International Committee for the Evaluation and Certification of Laboratory Animals) standard. The research protocol was approved by the Ethics Committee of The Fourth Hospital of Harbin Medical University (2023-DWSYLLCZ-49).

Acknowledgment

Not applicable.

Funding

This research was funded by the Heilongjiang Provincial Postdoctoral Research Startup Fund (LBH-Q21112).

Conflict of Interest

The authors declare no conflict of interest.

References

- [1] Su L. Comment on “Plasma alkylresorcinol metabolite, a biomarker of whole-grain wheat and rye intake, and risk of ischemic stroke: a case-control study”. *The American Journal of Clinical Nutrition*. 2019; 110: 524. <https://doi.org/10.1093/ajcn/nqz083>.
- [2] Avan A, Digaleh H, Di Napoli M, Stranges S, Behrouz R, Shojaeianbabaei G, *et al.* Socioeconomic status and stroke incidence, prevalence, mortality, and worldwide burden: an ecological analysis from the Global Burden of Disease Study 2017. *BMC Medicine*. 2019; 17: 191. <https://doi.org/10.1186/s12916-019-1397-3>.
- [3] Benjamin EJ, Muntner P, Alonso A, Bittencourt MS, Callaway CW, Carson AP, *et al.* Heart Disease and Stroke Statistics-2019 Update: A Report From the American Heart Association. *Circulation*. 2019; 139: e56–e528. <https://doi.org/10.1161/CIR.0000000000000659>.
- [4] Ji YB, Gao Q, Tan XX, Huang XW, Ma YZ, Fang C, *et al.* Lithium alleviates blood-brain barrier breakdown after cerebral ischemia and reperfusion by upregulating endothelial Wnt/ β -catenin signaling in mice. *Neuropharmacology*. 2021; 186: 108474. <https://doi.org/10.1016/j.neuropharm.2021.108474>.
- [5] Zhu T, Wang L, Tian F, Zhao X, Pu XP, Sun GB, *et al.* Anti-ischemia/reperfusion injury effects of notoginsenoside R1 on small molecule metabolism in rat brain after ischemic stroke as visualized by MALDI-MS imaging. *Biomedicine & Pharmacotherapy = Biomedecine & Pharmacotherapie*. 2020; 129: 110470. <https://doi.org/10.1016/j.biopha.2020.110470>.
- [6] Ran X, Xu T, Ruan H, Wang X, Zhang Q. Tissue Kallikrein supplementation in ischemic phase protects the neurovascular unit and attenuates reperfusion-induced injury in ischemic stroke. *Pharmacological Research*. 2024; 209: 107435. <https://doi.org/10.1016/j.phrs.2024.107435>.
- [7] Lu M, Liu J, Wu X, Zhang Z. Ciprofol: A Novel Alternative to Propofol in Clinical Intravenous Anesthesia? *BioMed Research International*. 2023; 2023: 7443226. <https://doi.org/10.1155/2023/7443226>.

- [8] Zhong J, Zhang J, Fan Y, Zhu M, Zhao X, Zuo Z, *et al.* Efficacy and safety of Ciprofol for procedural sedation and anesthesia in non-operating room settings. *Journal of Clinical Anesthesia*. 2023; 85: 111047. <https://doi.org/10.1016/j.jclinane.2022.111047>.
- [9] Liu X, Ren M, Zhang A, Huang C, Wang J. Nrf2 attenuates oxidative stress to mediate the protective effect of ciprofol against cerebral ischemia-reperfusion injury. *Functional & Integrative Genomics*. 2023; 23: 345. <https://doi.org/10.1007/s10142-023-01273-z>.
- [10] Makaryus R, Lee H, Yu M, Zhang S, Smith SD, Rebecchi M, *et al.* The metabolomic profile during isoflurane anesthesia differs from propofol anesthesia in the live rodent brain. *Journal of Cerebral Blood Flow and Metabolism: Official Journal of the International Society of Cerebral Blood Flow and Metabolism*. 2011; 31: 1432–1442. <https://doi.org/10.1038/jcbfm.2011.1>.
- [11] Li W, Shao C, Li C, Zhou H, Yu L, Yang J, *et al.* Metabolomics: A useful tool for ischemic stroke research. *Journal of Pharmaceutical Analysis*. 2023; 13: 968–983. <https://doi.org/10.1016/j.jpha.2023.05.015>.
- [12] Wu Z, Qian S, Zhao L, Zhang Z, Song C, Chen L, *et al.* Metabolomics-based study of the potential interventional effects of Xiao-Xu-Ming Decoction on cerebral ischemia/reperfusion rats. *Journal of Ethnopharmacology*. 2022; 295: 115379. <https://doi.org/10.1016/j.jep.2022.115379>.
- [13] Zhan Q, Thakur K, Feng JY, Zhu YY, Zhang JG, Wei ZJ. LC-MS based metabolomics analysis of okara fermented by *Bacillus subtilis* DC-15: Insights into nutritional and functional profile. *Food Chemistry*. 2023; 413: 135656. <https://doi.org/10.1016/j.foodchem.2023.135656>.
- [14] Longa EZ, Weinstein PR, Carlson S, Cummins R. Reversible middle cerebral artery occlusion without craniectomy in rats. *Stroke*. 1989; 20: 84–91. <https://doi.org/10.1161/01.str.20.1.84>.
- [15] Lasarzik I, Winkelheide U, Stallmann S, Orth C, Schneider A, Tresch A, *et al.* Assessment of postischemic neurogenesis in rats with cerebral ischemia and propofol anesthesia. *Anesthesiology*. 2009; 110: 529–537. <https://doi.org/10.1097/ALN.0b013e318195b4fe>.
- [16] Sugawara T, Ayer R, Jadhav V, Zhang JH. A new grading system evaluating bleeding scale in filament perforation subarachnoid hemorrhage rat model. *Journal of Neuroscience Methods*. 2008; 167: 327–334. <https://doi.org/10.1016/j.jneumeth.2007.08.004>.
- [17] Meng F, Fan L, Sun L, Yu Q, Wang M, Sun C. Serum biomarkers of the calcium-deficient rats identified by metabolomics based on UPLC/Q-TOF MS/MS. *Nutrition & Metabolism*. 2020; 17: 99. <https://doi.org/10.1186/s12986-020-00507-2>.
- [18] Stepanova A, Sosunov S, Niatetskaya Z, Konrad C, Starkov AA, Manfredi G, *et al.* Redox-Dependent Loss of Flavin by Mitochondrial Complex I in Brain Ischemia/Reperfusion Injury. *Antioxidants & Redox Signaling*. 2019; 31: 608–622. <https://doi.org/10.1089/ars.2018.7693>.
- [19] Kahl A, Stepanova A, Konrad C, Anderson C, Manfredi G, Zhou P, *et al.* Critical Role of Flavin and Glutathione in Complex I-Mediated Bioenergetic Failure in Brain Ischemia/Reperfusion Injury. *Stroke*. 2018; 49: 1223–1231. <https://doi.org/10.1161/STROKEAHA.117.019687>.
- [20] Liu D, Huang J, Gao S, Jin H, He J. A temporo-spatial pharmacometabolomics method to characterize pharmacokinetics and pharmacodynamics in the brain microregions by using ambient mass spectrometry imaging. *Acta Pharmaceutica Sinica*. B. 2022; 12: 3341–3353. <https://doi.org/10.1016/j.apsb.2022.03.018>.
- [21] Liao J, Li M, Huang C, Yu Y, Chen Y, Gan J, *et al.* Pharmacodynamics and Pharmacokinetics of HSK3486, a Novel 2,6-Disubstituted Phenol Derivative as a General Anesthetic. *Frontiers in Pharmacology*. 2022; 13: 830791. <https://doi.org/10.3389/fphar.2022.830791>.
- [22] Liu Y, Peng Z, Liu S, Yu X, Zhu D, Zhang L, *et al.* Efficacy and Safety of Ciprofol Sedation in ICU Patients Undergoing Mechanical Ventilation: A Multicenter, Single-Blind, Randomized, Noninferiority Trial. *Critical Care Medicine*. 2023; 51: 1318–1327. <https://doi.org/10.1097/CCM.0000000000005920>.
- [23] Chen, Q, Zhou T, Yuan JJ, Xiong XY, Liu XH, Qiu ZM, *et al.* Metabolomics profiling to characterize cerebral ischemia-reperfusion injury in mice. *Frontiers in Pharmacology*. 2023; 14: 1091616. <https://doi.org/10.3389/fphar.2023.1091616>.
- [24] Zhou H, Lin B, Yang J, Wei X, Fu W, Ding Z, *et al.* Analysis of the mechanism of Buyang Huanwu Decoction against cerebral ischemia-reperfusion by multi-omics. *Journal of Ethnopharmacology*. 2023; 305: 116112. <https://doi.org/10.1016/j.jep.2022.116112>.
- [25] Liu C, Zhang J, Mao K, Xu H, He Y. Astragalus membranaceus-Carthus tinctorius herb pair antagonizes parthanatos in cerebral ischemia/reperfusion injury via regulating PARP-1/TAX1BP1-mediated mitochondrial respiratory chain complex I. *Journal of Ethnopharmacology*. 2025; 340: 119260. <https://doi.org/10.1016/j.jep.2024.119260>.
- [26] Zhao, D, Zhang X, Jin WF, Huang P, Wan H, He Y. Efficacy of Astragalus membranaceus-Carthus tinctorius in cerebral ischemia/reperfusion injury: Insights from metabolomics and mass spectrometry imaging. *Phytomedicine*. 2024; 133: 155881. <https://doi.org/10.1016/j.phymed.2024.155881>.
- [27] Zhou P, Zhou L, Shi Y, Li Z, Liu L, Zuo L, *et al.* Neuroprotective Effects of Danshen Chuanxiongqin Injection Against Ischemic Stroke: Metabolomic Insights by UHPLC-Q-Orbitrap HRMS Analysis. *Frontiers in Molecular Biosciences*. 2021; 8: 630291. <https://doi.org/10.3389/fmolb.2021.630291>.
- [28] Ren JX, Li C, Yan XL, Qu Y, Yang Y, Guo ZN. Crosstalk between Oxidative Stress and Ferroptosis/Oxytosis in Ischemic Stroke: Possible Targets and Molecular Mechanisms. *Oxidative Medicine and Cellular Longevity*. 2021; 2021: 6643382. <https://doi.org/10.1155/2021/6643382>.
- [29] Wang SD, Fu YY, Han XY, Yong ZJ, Li Q, Hu Z, *et al.* Hyperbaric Oxygen Preconditioning Protects Against Cerebral Ischemia/Reperfusion Injury by Inhibiting Mitochondrial Apoptosis and Energy Metabolism Disturbance. *Neurochemical Research*. 2021; 46: 866–877. <https://doi.org/10.1007/s11064-020-03219-4>.
- [30] Jia J, Zhang H, Liang X, Dai Y, Liu L, Tan K, *et al.* Application of Metabolomics to the Discovery of Biomarkers for Ischemic Stroke in the Murine Model: a Comparison with the Clinical Results. *Molecular Neurobiology*. 2021; 58: 6415–6426. <https://doi.org/10.1007/s12035-021-02535-2>.
- [31] Jiang W, Gong L, Liu F, Ren Y, Mu J. Alteration of Gut Microbiome and Correlated Lipid Metabolism in Post-Stroke Depression. *Frontiers in Cellular and Infection Microbiology*. 2021; 11: 663967. <https://doi.org/10.3389/fcimb.2021.663967>.
- [32] Jung JY, Lee HS, Kang DG, Kim NS, Cha MH, Bang OS, *et al.* 1H-NMR-based metabolomics study of cerebral infarction. *Stroke*. 2011; 42: 1282–1288. <https://doi.org/10.1161/STROKEAHA.110.598789>.
- [33] Fernie AR, Carrari F, Sweetlove LJ. Respiratory metabolism: glycolysis, the TCA cycle and mitochondrial electron transport. *Current Opinion in Plant Biology*. 2004; 7: 254–261. <https://doi.org/10.1016/j.pbi.2004.03.007>.
- [34] O'Carroll SM, Peace CG, Toller-Kawahisa JE, Min Y, Hooffman A, Charki S, *et al.* Itaconate drives mRNA-mediated type I interferon production through inhibition of succinate dehydrogenase. *Nature Metabolism*. 2024; 6: 2060–2069. <https://doi.org/10.1038/s42255-024-01145-1>.
- [35] Mottahedin A, Prag HA, Dannhorn A, Mair R, Schmidt C, Yang M, *et al.* Targeting succinate metabolism to decrease brain injury

- upon mechanical thrombectomy treatment of ischemic stroke. *Redox Biology*. 2023; 59: 102600. <https://doi.org/10.1016/j.redox.2023.102600>.
- [36] da Silva-Candal A, Pérez-Díaz A, Santamaría M, Correa-Paz C, Rodríguez-Yáñez M, Ardá A, *et al*. Clinical validation of blood/brain glutamate grabbing in acute ischemic stroke. *Annals of Neurology*. 2018; 84: 260–273. <https://doi.org/10.1002/ana.25286>.
- [37] Kaushik P, Ali M, Tabassum H, Parvez S. Post-ischemic administration of dopamine D2 receptor agonist reduces cell death by activating mitochondrial pathway following ischemic stroke. *Life Sciences*. 2020; 261: 118349. <https://doi.org/10.1016/j.lfs.2020.118349>.
- [38] Curtabbi A, Guarás A, Cabrera-Alarcón JL, Rivero M, Calvo E, Rosa-Moreno M, *et al*. Regulation of respiratory complex I assembly by FMN cofactor targeting. *Redox Biology*. 2024; 69: 103001. <https://doi.org/10.1016/j.redox.2023.103001>.
- [39] Suwannasom N, Kao I, Pruß A, Georgieva R, Bäuml H. Riboflavin: The Health Benefits of a Forgotten Natural Vitamin. *International Journal of Molecular Sciences*. 2020; 21: 950. <https://doi.org/10.3390/ijms21030950>.
- [40] Jin C, Yao Y, Yonezawa A, Imai S, Yoshimatsu H, Otani Y, *et al*. Riboflavin Transporters RFVT/SLC52A Mediate Translocation of Riboflavin, Rather than FMN or FAD, across Plasma Membrane. *Biological & Pharmaceutical Bulletin*. 2017; 40: 1990–1995. <https://doi.org/10.1248/bpb.b17-00292>.
- [41] Henriques BJ, Lucas TG, Gomes CM. Therapeutic Approaches Using Riboflavin in Mitochondrial Energy Metabolism Disorders. *Current Drug Targets*. 2016; 17: 1527–1534. <https://doi.org/10.2174/1389450117666160813180812>.
- [42] Zhang C, Wu G. Recent advances in fluorescent probes for ATP imaging. *Talanta*. 2024; 279: 126622. <https://doi.org/10.1016/j.talanta.2024.126622>.
- [43] Lautrup S, Sinclair DA, Mattson MP, Fang EF. NAD⁺ in Brain Aging and Neurodegenerative Disorders. *Cell Metabolism*. 2019; 30: 630–655. <https://doi.org/10.1016/j.cmet.2019.09.001>.
- [44] Yoval-Sánchez B, Ansari F, James J, Niatetskaya Z, Sosunov S, Filipenko P, *et al*. Redox-dependent loss of flavin by mitochondria complex I is different in brain and heart. *Redox Biology*. 2022; 51: 102258. <https://doi.org/10.1016/j.redox.2022.102258>.
- [45] Zhang M, Chen H, Zhang W, Liu Y, Ding L, Gong J, *et al*. Biomimetic Remodeling of Microglial Riboflavin Metabolism Ameliorates Cognitive Impairment by Modulating Neuroinflammation. *Advanced Science (Weinheim, Baden-Württemberg, Germany)*. 2023; 10: e2300180. <https://doi.org/10.1002/advs.202300180>.
- [46] Fiedorczuk K, Letts JA, Degliesposti G, Kaszuba K, Skehel M, Sazanov LA. Atomic structure of the entire mammalian mitochondrial complex I. *Nature*. 2016; 538: 406–410. <https://doi.org/10.1038/nature19794>.
- [47] Almeida A, Allen KL, Bates TE, Clark JB. Effect of reperfusion following cerebral ischaemia on the activity of the mitochondrial respiratory chain in the gerbil brain. *Journal of Neurochemistry*. 1995; 65: 1698–1703. <https://doi.org/10.1046/j.1471-4159.1995.65041698.x>.
- [48] Lan X, Wang Q, Liu Y, You Q, Wei W, Zhu C, *et al*. Isoliquiritigenin alleviates cerebral ischemia-reperfusion injury by reducing oxidative stress and ameliorating mitochondrial dysfunction via activating the Nrf2 pathway. *Redox Biology*. 2024; 77: 103406. <https://doi.org/10.1016/j.redox.2024.103406>.
- [49] Cogliati S, Frezza C, Soriano ME, Varanita T, Quintana-Cabrera R, Corrado M, *et al*. Mitochondrial cristae shape determines respiratory chain supercomplexes assembly and respiratory efficiency. *Cell*. 2013; 155: 160–171. <https://doi.org/10.1016/j.cell.2013.08.032>.